Journal of Sound and Vibration (1999) **227**(3), 587–609
Article No. jsvi.1999.2356, available online at http://www.idealibrary.com on IDEAL®

VISCOTHERMAL WAVE PROPAGATION INCLUDING ACOUSTO-ELASTIC INTERACTION, PART II: APPLICATIONS

W. M. BELTMAN

University of Twente, Department of Mechanical Engineering, P.O. Box 217, 7500 *AE Enschede, The Netherlands*

(*Received* 15 *December* 1998, *and in final form* 6 *May* 1999)

In Part I of the present paper a parameter analysis showed that the most efficient model to describe viscothermal wave propagation is the low reduced frequency model. In order to demonstrate the wide range of applicability of the low reduced frequency model, a number of examples from the literature are discussed in Part II. An overview of fundamental solutions and general applications is given. Because the models are all written in terms of dimensionless parameters and solutions for various co-ordinate systems are given, this paper also serves as a solution overview.

1. INTRODUCTION

In Part I of the present paper an overview of theories for viscothermal wave propagation was presented. As a next step, the theory is applied to present solutions for the behaviour of spherical resonators, the propagation of sound in tubes, the behaviour of miniaturized transducers and squeeze film damping between flexible plates or membranes. Analytical solutions for the full model were obtained for a spherical geometry, a circular tube geometry and a layer geometry. The results of these models are compared with the results from simpler models, like the low reduced frequency model. All solutions are written in terms of dimensionless parameters. The use of these parameters leads to some interesting observations.

The author would like to stress that it is not his intention to give an extensive and very detailed description of all the aspects for each application. The present range of applications covers the general application field of linear viscothermal models. Furthermore, solutions are presented for a range of geometries. Thus, the main aim of this paper is to present an *application overview* and a *solution overview* of linear viscothermal models. The theory and the solutions are quite general and can easily be applied to other situations, because the expressions are all written in terms of dimensionless parameters.

0022-460X/99/430587 + 23 $30.00/0

2. SPHERICAL RESONATOR

2.1. INTRODUCTION

Spherical resonators are used to determine the properties of gases, such as the speed of sound, with a high degree of accuracy, see e.g. the paper by Moldover *et al.* [1]. In Figure 1, a schematic drawing is presented of a spherical resonator.

The sphere consists of two parts that are bolted together. The acoustic eigenfrequencies of the enclosed volume are used to determine the properties of the gas under different conditions. Because of the spherical geometry, an analytical solution can be obtained for the full linearized Navier–Stokes model as will be described in sections 2.2–2.5. However, the resonator contains a number of small disturbances: vent holes, transducers, transducer holes and a source. Although both parts of the shell are firmly bolted together, a small seam can remain between the two parts. In order to account for the presence of these disturbances, some suggestions to extend the model are introduced in section 2.6. Finally, an example with argon as a gas will be presented in section 2.7.

The derivation of the equations is based on the work by Moldover *et al.* [1]. The spherical resonator was also described by Bruneau *et al.* [2, 3], and Mehl [4–6]. The models were rewritten in terms of dimensionless quantities for the present study.

2.2. BASIC EQUATIONS

In order to solve the full linearized Navier–Stokes model, two *scalar wave equations* and one *vector wave equation* have to be solved (see Part I of the present paper). In a spherical co-ordinate system (r, θ, ϕ)

$$[\Delta + k_a^2]\, T_a = 0 \qquad [\Delta + k_h^2]\, T_h = 0 \qquad [\Delta + k_v^2]\, \mathbf{v}_v = \mathbf{0}. \tag{1}$$

A list of nomenclature is given in the Appendix.

2.3. SOLUTION OF THE SCALAR WAVE EQUATIONS

The solution of the scalar wave equations can be obtained by a straightforward separation of variables,

$$T_a = \mathrm{j}_n(k_a r)\mathrm{Y}_{mn}(\theta, \phi), \qquad T_h = \mathrm{j}_n(k_h r)\mathrm{Y}_{mn}(\theta, \phi), \tag{2}$$

where $\mathrm{Y}_{mn}(\theta, \phi)$ is a spherical harmonic function and $\mathrm{j}_n(k_a r)$ is a spherical Bessel function. The spherical Bessel function is related to the fractional Bessel function according to Abramovitz and Stengun [7]:

$$\mathrm{j}_n(k_a r) = \frac{1}{\sqrt{r}}\, \mathrm{J}_{n+1/2}(k_a r). \tag{3}$$

The solution for the temperature is

$$T = A_a \mathrm{j}_n(k_a r)\mathrm{Y}_{mn}(\theta, \phi) + A_h \mathrm{j}_n(k_h r)\mathrm{Y}_{mn}(\theta, \phi). \tag{4}$$

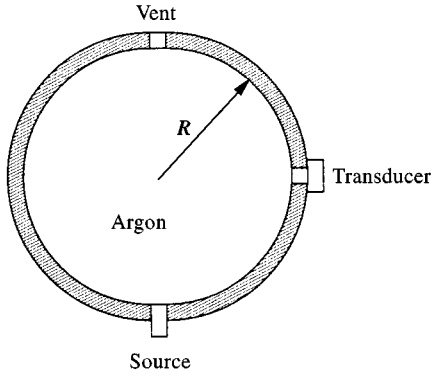

Figure 1. Schematic drawing of a spherical resonator.

The solenoidal velocity can be obtained from

$$\mathbf{v}_l = \mathbf{v}_{la} + \mathbf{v}_{lh} = \alpha_a A_a \nabla T_a + \alpha_h A_h \nabla T_h. \tag{5}$$

This gives

$$\begin{aligned}\mathbf{v}_l = &\left[\alpha_a A_a \frac{\partial \mathrm{j}_n(k_a r)}{\partial r} + \alpha_h A_h \frac{\partial \mathrm{j}_n(k_h r)}{\partial r}\right] \mathrm{Y}_{mn}(\theta, \phi)\mathbf{e}_r \\ &+ [\alpha_a A_a \mathrm{j}_n(k_a r) + \alpha_h A_h \mathrm{j}_n(k_h r)] \frac{1}{r} \frac{\partial \mathrm{Y}_{mn}(\theta, \phi)}{\partial \theta} \mathbf{e}_\theta \\ &+ [\alpha_a A_a \mathrm{j}_n(k_a r) + \alpha_h A_h \mathrm{j}_n(k_h r)] \frac{1}{r \sin(\theta)} \frac{\partial \mathrm{Y}_{mn}(\theta, \phi)}{\partial \phi} \mathbf{e}_\phi. \end{aligned} \tag{6}$$

The pressure is

$$p = \left[\frac{\gamma}{\gamma - 1}\right]\left[A_a\left[1 - \frac{\mathrm{i}k_a^2}{s^2\sigma^2}\right]\mathrm{j}_n(k_a r) + A_h\left[1 - \frac{\mathrm{i}k_h^2}{s^2\sigma^2}\right]\mathrm{j}_n(k_h r)\right]\mathrm{Y}_{mn}(\theta, \phi). \tag{7}$$

2.4. SOLUTION OF THE VECTOR WAVE EQUATION

The solution for the vector wave equation can be obtained from the solution of the scalar wave equation. For the present case the solution is (see the book by Morse and Feshbach [8])

$$\mathbf{v}_v = W_1 \nabla \times [\mathbf{e}_r r \mathrm{j}_n(k_v r)\mathrm{Y}_{mn}(\theta, \phi)] + W_2 \nabla \times \nabla \times [\mathbf{e}_r r \mathrm{j}_n(k_v r)\mathrm{Y}_{mn}(\theta, \phi)], \tag{8}$$

where W_1 and W_2 are constants that remain to be determined from the boundary conditions. After some algebra one obtains

$$\mathbf{v}_v = W_1[-r\mathrm{j}_n(k_v r)] \frac{1}{r \sin(\theta)} \frac{\partial \mathrm{Y}_{mn}(\theta, \phi)}{\partial \phi} \mathbf{e}_\theta + W_1[r\mathrm{j}_n(k_v r)] \frac{1}{r} \frac{\partial \mathrm{Y}_{mn}(\theta, \phi)}{\partial \theta} \mathbf{e}_\phi$$

$$+ W_2\left[\frac{n(n+1)}{r}\,\mathrm{j}_n(k_v r)\right]\mathrm{Y}_{mn}(\theta,\phi)\mathbf{e}_r + W_2\left[\frac{\partial}{\partial r}\,(r\mathrm{j}_n(k_v r))\right]\frac{1}{r}\frac{\partial \mathrm{Y}_{mn}(\theta,\phi)}{\partial\theta}\,\mathbf{e}_\theta$$

$$+ W_2\left[\frac{\partial}{\partial r}\,(r\mathrm{j}_n(k_v r))\right]\frac{1}{r\sin(\theta)}\frac{\partial \mathrm{Y}_{mn}(\theta,\phi)}{\partial\phi}\,\mathbf{e}_\phi. \tag{9}$$

2.5. RIGID SPHERE WITH ISOTHERMAL WALLS

The boundary conditions for the present case for $r = 1$ are

$$T = 0, \qquad \mathbf{v} = \mathbf{v}_l + \mathbf{v}_v = \mathbf{0}. \tag{10}$$

The following equation for the spherical resonator is obtained:

$$\left[1 - \frac{\alpha_h}{\alpha_a}\right]\left[\frac{n(n+1)}{1 + (1/\mathrm{j}_n(k_v))(\partial \mathrm{j}_n(k_v r)/\partial r)|_{r=1}}\right]$$

$$= \frac{1}{\mathrm{j}_n(k_a)}\frac{\partial \mathrm{j}_n(k_a r)}{\partial r}\bigg|_{r=1} - \left(\frac{\alpha_h}{\alpha_a}\right)\frac{1}{\mathrm{j}_n(k_h)}\frac{\partial \mathrm{j}_n(k_h r)}{\partial r}\bigg|_{r=1}. \tag{11}$$

The eigenfrequencies of the gas in the resonator can be calculated from this equation. In experiments, a frequency response function is measured. The frequency response of the resonator is calculated by expressing the internal acoustic field in terms of the acoustic eigenmodes. The participation factors can then be calculated; see e.g. reference [1].

2.6. MODEL EXTENSIONS

As stated before, the derivation of the equations is based on the work by Moldover *et al.* [1]. The spherical resonator was also described by Bruneau *et al.* [2, 3] and Mehl [4–6]. The models were rewritten in terms of dimensionless quantities for the present study.

2.6.1. *Shell motion*

As a boundary condition, a zero velocity was imposed for the gas at the shell wall. The shell however can deform under the applied pressure. Mehl [4] developed a model which describes the shell behaviour in terms of an impedance. The effect of shell motion can thus be incorporated in the model by imposing the shell impedance as a boundary condition for the radial velocity and the pressure at the shell wall.

2.6.2. *Holes in the shell*

The holes will affect the acoustic field inside the resonator. One can distinguish several types of holes, depending on the type of termination. For vent holes, the

circular tube is terminated by a radiation or pressure release condition. For the transducer holes, the tube is terminated by the effective impedance of the transducer itself. The propagation of sound waves in a circular tube is governed by the dimensionless parameters. With these parameters, the most efficient model can be identified. The acoustic impedance of the tube with its termination can be calculated and thus the impedance at the entrance of the tube is known. As a consequence, there is a non-uniform boundary impedance condition for the gas in the resonator.

2.6.3. *Seam*

A small gap at the junction between the two hemispheres can affect the acoustical properties of the resonator. In this case, one deals with the propagation of sound waves between parallel surfaces. Again, based on the dimensionless parameters for this layer geometry one can easily identify the model that should be used. The effective impedance of the gap between the hemispheres can then be calculated.

2.7. EXAMPLE: EIGENFREQUENCIES OF SPHERICAL RESONATOR

The properties of the argon gas and the spherical resonator are (according to the case described by Moldover *et al.* [1])

$$c_0 = 319 \text{ m/s}, \qquad \rho_0 = 1{\cdot}60 \text{ kg/m}^3, \qquad C_p = 528 \text{ J/kgK}, \qquad \gamma = 5/3,$$
$$\lambda = 16{\cdot}7 \times 10^{-3} \text{ W/mk}, \qquad \mu = 22{\cdot}7 \times 10^{-6} \text{ Ns/m}^2,$$
$$\xi = 0, \qquad R = 0{\cdot}0635 \text{ m}. \tag{12}$$

The bulk viscosity is zero and the ratio of specific heats is equal to $\frac{5}{3}$ for a monatomic (ideal) gas like argon. The eigenfrequencies of the resonator were calculated with a simple numerical procedure. The eigenfrequencies can be divided into groups. For each value of n there are several solutions to the equation. The solutions are denoted here as "ns", where n is the order of the spherical Bessel function and s is the sth root. The roots are arranged in ascending order. The results for the $n = 0$, 1 and 2 modes are given in Table 1.

The table shows that the eigenfrequencies for the full model are complex. The imaginary part however is very small compared to the real part. The real part of the frequency is almost equal to the frequency that is obtained with the wave equation. The viscous and thermal effects seem to have only a small effect on the acoustical eigenfrequencies of the resonator. However, the shifts in frequency have to be related to the accuracy of the experiment. In fact, according to the literature a frequency shift of several Hz can be denoted as "significant". The resonance half-width, which is equal to the imaginary part of the eigenfrequency, is measured in the experiments. The viscous and thermal effects partly determine the imaginary component of the frequency. For a good model, however, the motion of the shell wall must be included, for example by using the impedance approach.

TABLE 1

Eigenfrequencies of a spherical resonator

"*ns*"	Eigenfrequency (Hz)	
	Wave equation	Full model
01	0	0
02	3593	3592 + 0·802i
03	6177	6175 + 1·073i
04	8718	8717 + 1·305i
11	1664	1663 + 1·587i
12	4750	4748 + 1·054i
13	7360	7359 + 1·246i
14	9918	9916 + 1·449i
21	2630	2628 + 1·988i
22	5817	5816 + 1·363i
23	8482	8481 + 1·460i
24	11069	11067 + 1·623i

3. CIRCULAR TUBES

3.1. INTRODUCTION

The propagation of sound waves in tubes was already investigated by Kirchhoff and Rayleigh; see, e.g. reference [9]. A large amount of literature is available on this subject, dealing with full linearized Navier–Stokes models, simplified models and low reduced frequency models. For an overview of models in terms of dimensionless parameters the reader is referred to the paper by Tijdeman [10], in which also numerical results for the fundamental mode ($m = 0$) were presented which took into account the influence of thermal effects. The theory, presented in Part I of the present paper, will now be applied to describe the propagation of sound waves in circular tubes. A solution for the full linearized Navier–Stokes model is given. Extending the work of Tijdeman, the present solution includes circumferential harmonic waves of integer order m and the effects of bulk viscosity. The results for the case of $m = 0$ and zero bulk viscosity are compared with the results presented by Tijdeman.

3.2. FULL LINEARIZED NAVIER–STOKES MODEL

3.2.1. *Basic equations*

In order to solve the full linearized Navier–Stokes model, two *scalar wave equations* and one *vector wave equation* have to be solved (see Part I of the present paper). In a cylindrical co-ordinate system (r, θ, x)

$$[\Delta + k_a^2]\, T_a = 0, \qquad [\Delta + k_h^2]\, T_h = 0, \qquad [\Delta + k_v^2]\mathbf{v}_v = \mathbf{0}. \tag{13}$$

3.2.2. *Solution of the scalar wave equation*

The solution of the scalar wave equations can be obtained by a straightforward separation of variables,

$$T_a = \mathrm{J}_m(k_{ar}r)\,f_m(\theta, x), \qquad T_h = \mathrm{J}_m(k_{hr}r)\,f_m(\theta, x), \tag{14}$$

where

$$f_m(\theta, x) = [C_1\mathrm{e}^{-\mathrm{i}m\theta} + C_2\mathrm{e}^{\mathrm{i}m\theta}][C_3\mathrm{e}^{-\Gamma x} + \mathrm{C}_4\mathrm{e}^{\Gamma x}],$$
$$k_{ar} = \sqrt{k_a^2 + k^2\Gamma^2}, \qquad k_{hr} = \sqrt{k_h^2 + k^2\Gamma^2}. \tag{15}$$

The function $f_m(\theta, x)$ consists of circumferential harmonics of integer order m that are travelling in the $+x$ and the $-x$-directions. The quantity Γ is the *propagation constant*. The solution for the temperature is

$$T = A_a\mathrm{J}_m(k_{ar}r)\,f_m(\theta, x) + A_h\mathrm{J}_m(k_{hr}r)\,f_m(\theta, x). \tag{16}$$

The solenoidal velocity can be obtained from

$$\mathbf{v}_l = \mathbf{v}_{la} + \mathbf{v}_{lh} = \alpha_a A_a \boldsymbol{\nabla} T_a + A_h\alpha_h \boldsymbol{\nabla} T_h. \tag{17}$$

This gives

$$\mathbf{v}_l = \left[\alpha_a A_a \frac{\partial \mathrm{J}_m(k_{ar}r)}{\partial r} + \alpha_h A_h \frac{\partial \mathrm{J}_m(k_{hr}r)}{\partial r}\right] f_m(\theta, x)\mathbf{e}_r$$
$$+ [\alpha_a A_a \mathrm{J}_m(k_{ar}r) + \alpha_h A_h \mathrm{J}_m(k_{hr}r)]\,\frac{1}{r}\frac{\partial f_m(\theta, x)}{\partial \theta}\,\mathbf{e}_\theta$$
$$+ [\alpha_a A_a \mathrm{J}_m(k_{ar}r) + \alpha_h A_h \mathrm{J}_m(k_{hr}r)]\,k\frac{\partial f_m(\theta, x)}{\partial x}\,\mathbf{e}_x. \tag{18}$$

The pressure is

$$p = \left[\frac{\gamma}{\gamma - 1}\right]\left[A_a\left[1 - \frac{\mathrm{i}k_a^2}{s^2\sigma^2}\right]\mathrm{J}_m(k_{ar}r) + A_h\left[1 - \frac{\mathrm{i}k_h^2}{s^2\sigma^2}\right]\mathrm{J}_m(k_{hr}r)\right] f_m(\theta, x). \tag{19}$$

3.2.3. *Solution of the vector wave equation*

The solution of the vector wave equation is (see the book by Morse and Feshbach [8])

$$\mathbf{v}_v = W_1\boldsymbol{\nabla} \times [\mathbf{e}_x\,\mathrm{J}_m(k_{vr}r)\,f_m(\theta, x)] + W_2\boldsymbol{\nabla} \times \boldsymbol{\nabla} \times [\mathbf{e}_x\mathrm{J}_m(k_{vr}r)\,f_m(\theta, x)], \tag{20}$$

where W_1 and W_2 are constants that remain to be determined from the boundary conditions, and

$$k_{vr} = \sqrt{k_v^2 + k^2\Gamma^2}. \tag{21}$$

After some algebra one obtains

$$\mathbf{v}_v = W_1[\mathrm{J}_m(k_{vr}r)]\frac{1}{r}\frac{\partial f_m(\theta,x)}{\partial\theta}\mathbf{e}_r - W_1\left[\frac{\mathrm{J}_m(k_{vr}r)}{\partial r}\right]f_m(\theta,x)\mathbf{e}_\theta$$
$$+ W_2[(k_v^2 + k^2\Gamma^2)\mathrm{J}_m(k_{vr}r)]\,f_m(\theta,x)\mathbf{e}_x + W_2[\mathrm{J}_m(k_{vr}r)]k\frac{1}{r}\frac{\partial^2 f_m(\theta,x)}{\partial\theta\,\partial x}\mathbf{e}_\theta$$
$$+ W_2\left[\frac{\partial \mathrm{J}_m(k_{vr}r)}{\partial r}\right]k\frac{\partial f_m(\theta,x)}{\partial x}\mathbf{e}_x. \tag{22}$$

3.2.4. *Dispersion equation*

For a rigid tube with isothermal walls, the following boundary conditions apply for $r = 1$:

$$T = 0, \qquad \mathbf{v} = \mathbf{v}_v + \mathbf{v}_l = \mathbf{0}. \tag{23}$$

After some algebraic manipulations one obtains the following dispersion equation:

$$\left[1 - \frac{\alpha_h}{\alpha_a}\right]\frac{k_v^2}{k_v^2 + k^2\Gamma^2}\left[\frac{m^2}{(1/\mathrm{J}_m(k_{vr}))(\partial \mathrm{J}_m(k_{vr}r)/\partial r)}\bigg|_1 + \frac{k^2\Gamma^2}{k_v^2}\frac{1}{\mathrm{J}_m(k_{vr})}\frac{\partial \mathrm{J}_m(k_{vr}r)}{\partial r}\bigg|_1\right]$$
$$= \frac{1}{\mathrm{J}_m(k_{ar})}\frac{\partial \mathrm{J}_m(k_{ar}r)}{\partial r}\bigg|_1 - \frac{\alpha_h}{\alpha_a}\frac{\partial \mathrm{J}_m(k_{hr}r)/\partial r|_1}{\mathrm{J}_m(k_{hr})}. \tag{24}$$

For given values of the dimensionless parameters and the order m, the value of the (complex) propagation constant Γ can be solved for from this equation.

3.3. LOW REDUCED FREQUENCY MODEL

For a circular tube with isothermal walls, the low reduced frequency solution for the pressure (see Part I of the present paper) is

$$p = C_1 \mathrm{e}^{-\Gamma x} + C_2 \mathrm{e}^{\Gamma x}, \qquad \Gamma = \sqrt{\gamma/n(s\sigma)B(s)}, \tag{25, 26}$$

where

$$n(s\sigma) = \left[1 + \left[\frac{\gamma - 1}{\gamma}\right]B(s\sigma)\right]^{-1}, \qquad B(s) = \frac{\mathrm{J}_2(s\mathrm{i}\sqrt{\mathrm{i}})}{\mathrm{J}_0(s\mathrm{i}\sqrt{\mathrm{i}})}. \tag{27}$$

The propagation of waves is governed by the value of the propagation constant Γ. There are two waves: one travelling in the negative x-direction and one travelling in the positive x-direction. Note that the pressure is constant across the cross-section of the tube in the low reduced frequency model.

3.4. EXAMPLE: PROPAGATION CONSTANT

3.4.1. $m = 0$

Consider the case $m = 0$, i.e., there is no pressure variation in the circumferential direction. The full linearized Navier–Stokes model was used to calculate the value

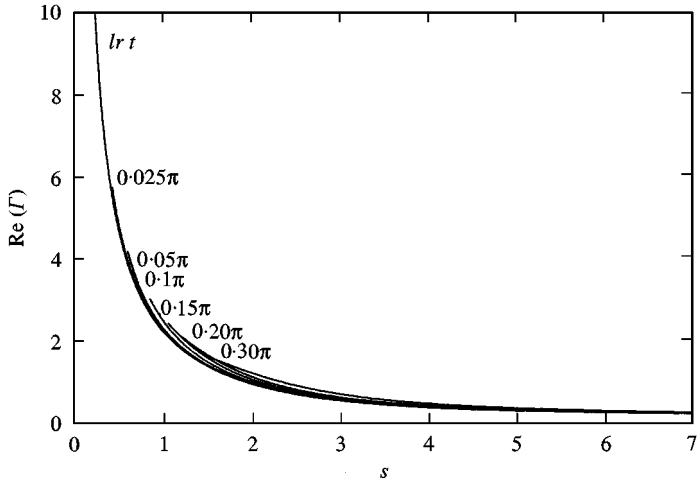

Figure 2. Real part of Γ for $\xi = 0$, $m = 0$ (first root), $k = 0{\cdot}025\pi$, $0{\cdot}05\pi$, $0{\cdot}1\pi$, $0{\cdot}15\pi$, $0{\cdot}2\pi$, $0{\cdot}3\pi$ and the low reduced frequency solution.

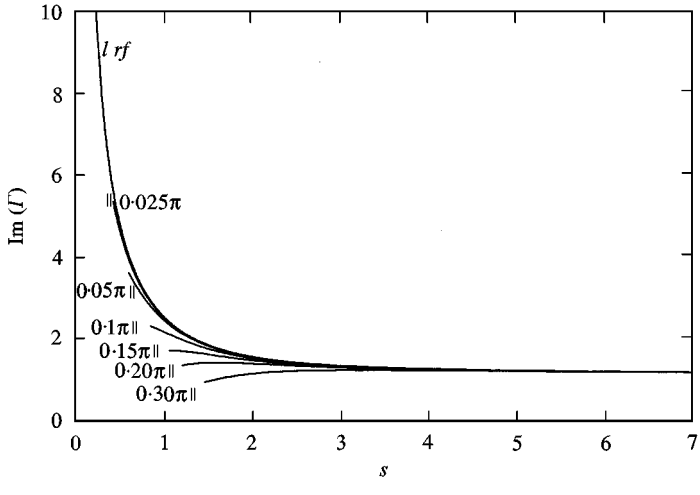

Figure 3. Imaginary part of Γ for $\xi = 0$, $m = 0$ (first root), $k = 0{\cdot}025\pi$, $0{\cdot}05\pi$, $0{\cdot}1\pi$, $0{\cdot}15\pi$, $0{\cdot}2\pi$, $0{\cdot}3\pi$ and the low reduced frequency solution.

of the propagation constant for different values of k and s. When $k \ll 1$ and $k/s \ll 1$ the solution of the full model should converge to the low reduced frequency solution for Γ. Note that the propagation constant does not depend on the value of the reduced frequency k in the low reduced frequency model.

The calculated values for $\xi = 0$ and $\xi = 0{\cdot}6$ for air under atmospheric conditions ($\gamma = 1{\cdot}4$ and $\sigma = \sqrt{0{\cdot}71}$) are given in Figures 2–5. The basic assumptions are valid only for $k/s < 0{\cdot}3\pi$ and $s > 2{\cdot}24k/s$. In the figures the curves are truncated at the point where these basic assumptions are violated. For each value of k and k/s there are several solutions of the dispersion equation, corresponding to different radial wave numbers. In all figures the first root is given. The results for the case $\xi = 0$ are identical to the results presented by Tijdeman [10]. The figures show that the bulk

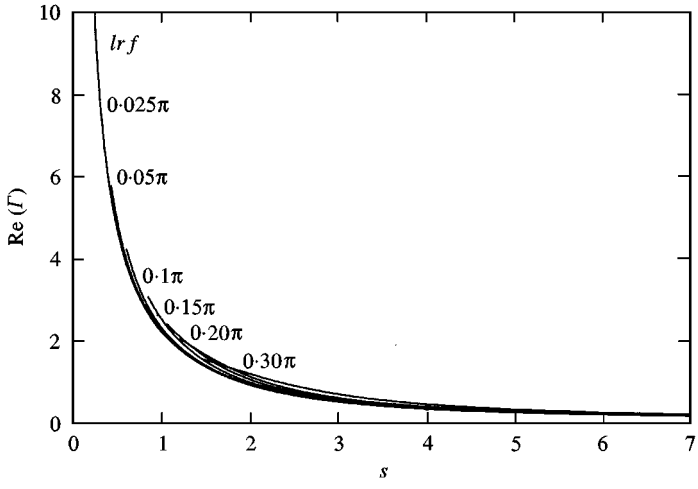

Figure 4. Real part of Γ for $\xi = 0{\cdot}6$, $m = 0$ (first root), $k = 0{\cdot}025\pi$, $0{\cdot}05\pi$, $0{\cdot}1\pi$, $0{\cdot}15\pi$, $0{\cdot}2\pi$, $0{\cdot}3\pi$ and the low reduced frequency solution.

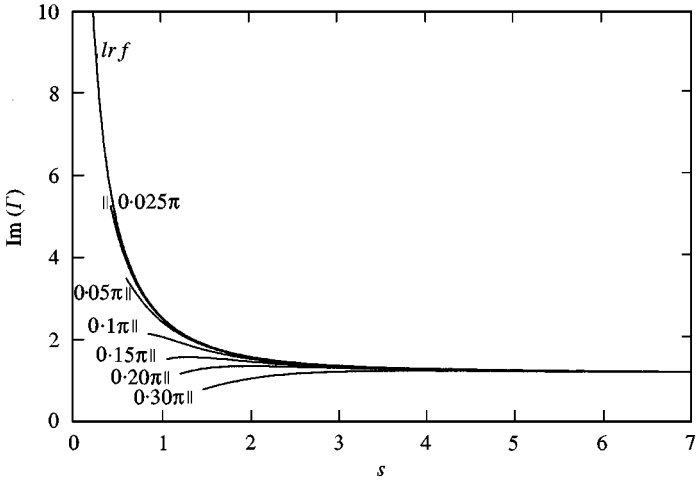

Figure 5. Imaginary part of Γ for $\xi = 0{\cdot}6$, $m = 0$ (first root), $k = 0{\cdot}025\pi$, $0{\cdot}05\pi$, $0{\cdot}1\pi$, $0{\cdot}15\pi$, $0{\cdot}2\pi$, $0{\cdot}3\pi$ and the low reduced frequency solution.

viscosity has only a small influence on the value of the propagation constant for low shear wave numbers. For small values of k and k/s the solution of the full linearized Navier–Stokes model converges to the low reduced frequency solution for Γ. Thus, for air under atmospheric conditions the low reduced frequency model is accurate. Under more extreme conditions, however, the results could be less accurate and the full linearized Navier–Stokes model must be used.

3.4.2. $m = 1$

In this case there is a harmonic variation of the pressure in the circumferential direction. The low reduced frequency model is not able to describe this "spiralizing"

type of wave because the pressure is assumed to be constant on a cross-section. In the acoustic non-dissipative case there is a cut-on frequency. For frequencies below the cut-on frequency the solution for Γ is purely real and the wave will die out exponentially in the axial direction. When the frequency exceeds the cut-on frequency, the solution for Γ is purely imaginary and the wave starts to propagate. The cut-on frequency increases with increasing radial wavenumber. The lowest cut-on frequency is calculated from $k = 1{\cdot}84$. For air under atmospheric conditions the basic assumptions require $k/s < 0{\cdot}3\pi$. Thus, the shear wave number must be larger than 2, which suggests that viscothermal effects will usually only be of minor importance for these waves. The solution for higher order circumferential modes including viscothermal effects can be calculated with the full linearized Navier–Stokes model. A detailed analysis of this topic, however, is not within the scope of the present study; see e.g. references [11–15].

4. MINIATURIZED TRANSDUCER

Consider a vibrating membrane, backed by a rigid electrode (see Figure 6). The membrane and the electrode entrap a thin layer of air. The air layer is surrounded by a large reservoir at the periphery.

The displacement of the membrane is zero at the edges, i.e., at $\bar{r} = R$. The layer thickness is $2h_0$. Because the layer is surrounded by a large reservoir the condition $p = 0$ is imposed at $\bar{r} = R$. The membrane is excited by a plane wave with magnitude $\bar{p}_i$ at $z = h_0$. Only the rotatory symmetric case will be considered in the present analysis. Typical operating ranges for this type of transducer are a layer thickness of the order of 10^{-5} m, a radius $R = 10^{-2}$ m and a frequency range of up to 100 kHz.

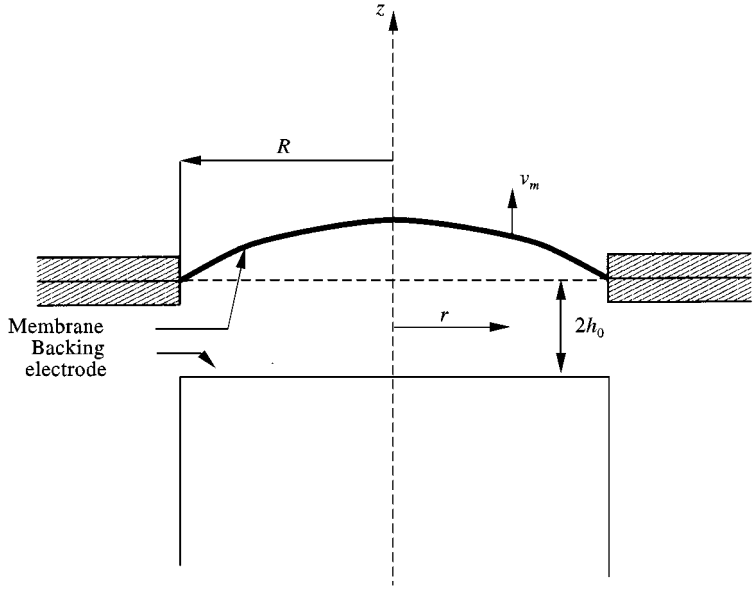

Figure 6. Miniaturized transducer.

4.1. FULL LINEARIZED NAVIER–STOKES SOLUTION

The basic equations for the problem are two scalar wave equations, one vector wave equation and the equation of motion for the membrane:

$$[\Delta + k_a^2]\,T_a = 0, \qquad [\Delta + k_h^2]\,T_h = 0,$$

$$[\Delta + k_v^2]\,\mathbf{v}_v = \mathbf{0}, \qquad \left[\Delta^r + \frac{k^2\Omega^2}{k_r^2}\right] v_m = -\,\mathrm{i}\,\frac{\Omega^2 \varepsilon k}{\gamma k_r^2}\,[p - p_i]. \tag{28}$$

Here k_a, k_h and k_v are the acoustic, entropic and rotational wave numbers, (see Part I of the present paper), v_m is the dimensionless membrane velocity in the z-direction and p_i is the dimensionless external incident pressure. The parameters k_r, Ω (a dimensionless frequency), ε (a coupling parameter) and the operators Δ and Δ^r are defined as

$$\Omega^2 = \frac{\omega^2 R^2 t_m \rho_m}{T_m}, \qquad k_r = \frac{\omega R}{c_0}, \qquad \varepsilon = \frac{\rho_0 h_0}{\rho_m t_m},$$

$$\Delta = k^2\frac{\partial^2}{\partial r^2} + k^2\frac{1}{r}\frac{\partial}{\partial r} + \frac{\partial^2}{\partial z^2}, \qquad \Delta^r = k^2\frac{\partial^2}{\partial r^2} + k^2\frac{1}{r}\frac{\partial}{\partial r}, \tag{29}$$

where t_m, T_m and ρ_m represent the thickness, the tension and the density of the membrane.

4.1.1. *Solution of the scalar wave equation*

After extensive algebra the following expressions for the temperatures are found:

$$T_a = \sum_{q=1,2,\ldots} \mathrm{J}_0\left(\frac{k_q}{k} r\right)[B_{aq}\sin(k_{aq}z) + A_{aq}\cos(k_{aq}z)],$$

$$T_h = \sum_{q=1,2,\ldots} \mathrm{J}_0\left(\frac{k_q}{k} r\right)[B_{hq}\sin(k_{hq}z) + A_{hq}\cos(k_{hq}z)]. \tag{30}$$

The solenoidal velocity can be obtained from†

$$\mathbf{v}_l = \mathbf{v}_{la} + \mathbf{v}_{lh} = \alpha_a \nabla T_a + \alpha_h \nabla T_h. \tag{31}$$

This gives

$$\begin{aligned}
\mathbf{v}_l = &\sum_{q=1,2,\ldots} -\frac{k_q}{k}\,\mathrm{J}_1\left(\frac{k_q}{k} r\right)\alpha_a[B_{aq}\sin(k_{aq}z) + A_{aq}\cos(k_{aq}z)]\,\mathbf{e}_r \\
&+ \sum_{q=1,2,\ldots} -\frac{k_q}{k}\,\mathrm{J}_1\left(\frac{k_q}{k} r\right)\alpha_h[B_{hq}\sin(k_{hq}z) + A_{hq}\cos(k_{hq}z)]\,\mathbf{e}_r \\
&+ \sum_{q=1,2,\ldots} \mathrm{J}_0\left(\frac{k_q}{k} r\right)\alpha_a[B_{aq}\cos(k_{aq}z) - A_{aq}\sin(k_{aq}z)]\,\mathbf{e}_z \\
&+ \sum_{q=1,2,\ldots} \mathrm{J}_0\left(\frac{k_q}{k} r\right)\alpha_h[B_{hq}\cos(k_{hq}z) - A_{hq}\sin(k_{hq}z)]\,\mathbf{e}_z,
\end{aligned} \tag{32}$$

†The constants A_a and A_h are contained in A_{aq}, B_{aq}, A_{hq} and B_{hq}.

where the different wave numbers are given by

$$k_{aq}^2 = k_a^2 - k_q^2, \qquad k_{hq}^2 = k_h^2 - k_q^2, \qquad k_{vq}^2 = k_v^2 - k_q^2. \tag{33}$$

The values of k_q are the roots of the equation

$$\mathrm{J}_0\left(\frac{k_q}{k}\, k_r\right) = 0. \tag{34}$$

The pressure is

$$p = \left[\frac{\gamma}{\gamma - 1}\right]\left[\left[1 - \frac{\mathrm{i}k_a^2}{s^2}\frac{1}{\sigma^2}\right]T_a + \left[1 - \frac{\mathrm{i}k_h^2}{s^2}\frac{1}{\sigma^2}\right]T_h\right]. \tag{35}$$

4.1.2. *Solution of the vector wave equation*

The rotational velocity is given by

$$\mathbf{v}_v = \sum_{q=1,2,\ldots} \frac{k_{vq}}{k_q}\,\mathrm{J}_1\left(\frac{k_q}{k}\, r\right)[A_{vq}\sin(k_{vq}z) - B_{vq}\cos(k_{vq}z)]\mathbf{e}_r$$

$$+ \sum_{q=1,2,\ldots} \mathrm{J}_0\left(\frac{k_q}{k}\, r\right)[B_{vq}\sin(k_{vq}z) + A_{vq}\cos(k_{vq}z)]\mathbf{e}_z. \tag{36}$$

4.1.3. *Solution of the problem*

There are six constants that remain to be determined: A_{aq}, A_{hq}, A_{vq}, B_{aq}, B_{hq}, and B_{vq}. The following conditions can be used to determine the values of these constants:

$$T = 0 \quad \text{for } z = \pm 1, \qquad p = 0 \quad \text{for } r = k_r,$$

$$[\mathbf{v}_l + \mathbf{v}_v]\cdot\mathbf{e}_r = 0 \quad \text{for } z = \pm 1, \qquad [\mathbf{v}_l + \mathbf{v}_v]\cdot\mathbf{e}_z = v_m \quad \text{for } z = 1.$$

The velocity of the membrane is

$$v_m = -\,\mathrm{i}\frac{\Omega^2\varepsilon k}{\gamma k_r^2}\frac{p_i k_r^2}{k^2\Omega^2}\left[\frac{\mathrm{J}_0((\Omega/k_r)r)}{\mathrm{J}_0(\Omega)} - 1\right]$$

$$-\,\mathrm{i}\frac{\Omega^2\varepsilon k}{\gamma k_r^2}\sum_{q=1,2,\ldots}\frac{\mathrm{J}_0((k_q/k)r)}{[(k^2\Omega^2/k_r^2) - k_q^2]}\{\Lambda_a[A_{aq}\cos(k_{aq}z) + B_{aq}\sin(k_{aq}z)]\}$$

$$-\,\mathrm{i}\frac{\Omega^2\varepsilon k}{\gamma k_r^2}\sum_{q=1,2,\ldots}\frac{\mathrm{J}_0((k_q/k)r)}{[(k^2\Omega^2/k_r^2) - k_q^2]}\{\Lambda_h[A_{hq}\cos(k_{hq}z) + B_{hq}\sin(k_{hq}z)]\}, \tag{37}$$

where the following symbols were used:

$$\Lambda_a = \left[\frac{\gamma}{\gamma - 1}\right]\left[1 - \frac{\mathrm{i}k_a^2}{s^2}\frac{1}{\sigma^2}\right], \qquad \Lambda_h = \left[\frac{\gamma}{\gamma - 1}\right]\left[1 - \frac{\mathrm{i}k_h^2}{s^2}\frac{1}{\sigma^2}\right]. \tag{38}$$

4.2. LOW REDUCED FREQUENCY SOLUTION

The low reduced frequency problem results in two coupled scalar equations:

$$[\Delta^r - k^2\Gamma^2]p = -\tfrac{1}{2}\mathrm{i}kn(s\sigma)\Gamma^2 v_m, \qquad \left[\Delta^r + \frac{k^2\Omega^2}{k_r^2}\right]v_m = -\,\mathrm{i}\,\frac{\Omega^2\varepsilon k}{\gamma k_r^2}[p - p_i]. \quad (39)$$

The solution is

$$p = \sum_{q=1,2,\ldots} A_q \mathrm{J}_0\left(\frac{k_q}{k}r\right), \qquad v_m = \sum_{q=1,2,\ldots} B_q \mathrm{J}_0\left(\frac{k_q}{k}r\right), \quad (40)$$

where the participation factors A_q and B_q are given by

$$A_q = \frac{\mathrm{i}kn(s\sigma)\Gamma^2}{2[k_q^2 + k^2\Gamma^2]}B_q,$$

$$B_q = -\,\mathrm{i} \times \frac{\Omega^2\varepsilon k}{\gamma k_r^2}\frac{-2p_i}{k_q k_r[(k^2\Omega^2/k_r^2) - k_q^2 + \dfrac{(kn(s\sigma)\Gamma^2}{2[k_q^2 + k^2\Gamma^2]}\cdot\dfrac{\Omega^2\varepsilon k}{\gamma k_r^2}\mathrm{J}_1(k_q/k)k_r)}. \quad (41)$$

4.3. EXAMPLE: MEMBRANE IMPEDANCE

As a test case, the impedance of the system is calculated. This test case was described by Plantier and Bruneau [16]. They used a full linearized Navier–Stokes model with simplified wave numbers. In the present analysis, however, the full expressions for the wave numbers are used, since the simplification of the wave numbers actually eliminates the need for a full model (see Part I of the present paper). The real and the imaginary parts of the impedance are defined in terms of the incident pressure $\bar{p}_i$ and the *average* membrane velocity $\langle\overline{v_m}\rangle$:

$$\bar{Z}_r = 10^{10}\log\left[\frac{(\mathrm{Re}(\bar{Z}))^2}{\bar{Z}_0^2}\right], \qquad \bar{Z}_i = 10^{10}\log\left[\frac{(\mathrm{Im}(\bar{Z}))^2}{\bar{Z}_0^2}\right],$$

$$\langle\overline{v_m}\rangle = \frac{1}{\pi R^2}\int_0^R \bar{v}_m 2\pi\bar{r}\,\mathrm{d}\bar{r}, \qquad \bar{Z} = \frac{\bar{p}_i}{\langle\bar{v}_m\rangle}, \qquad \bar{Z}_0 = 1\times10^4\ \mathrm{Ns/m^3}. \quad (42)$$

The following properties were used (according to Plantier and Bruneau [16]):

$$R = 1{\cdot}37\times10^{-2}\ \mathrm{m}, \qquad \rho_m = 4{\cdot}5\times10^3\ \mathrm{kg/m^3}, \qquad T_m = 6{\cdot}2\times10^3\ \mathrm{N/m},$$

$$t_m = 12{\cdot}7\times10^{-6}\ \mathrm{m}, \qquad 2h_0 = 25{\cdot}4\times10^{-6}\ \mathrm{m}, \qquad \rho_0 = 1{\cdot}2\ \mathrm{kg/m^3},$$

$$\lambda = 25{\cdot}6\times10^{-3}\ \mathrm{W/mK}, \qquad C_v = 716\ \mathrm{J/kgK}, \qquad C_p = 1004\ \mathrm{J/kgK},$$

$$c_0 = 340\ \mathrm{m/s}, \qquad \mu = 18{\cdot}2\times10^{-6}\ \mathrm{Ns/m^2}, \qquad \xi = 0{\cdot}6. \quad (43)$$

The results for the full linearized Navier–Stokes model and the low reduced frequency model are plotted in Figure 7.

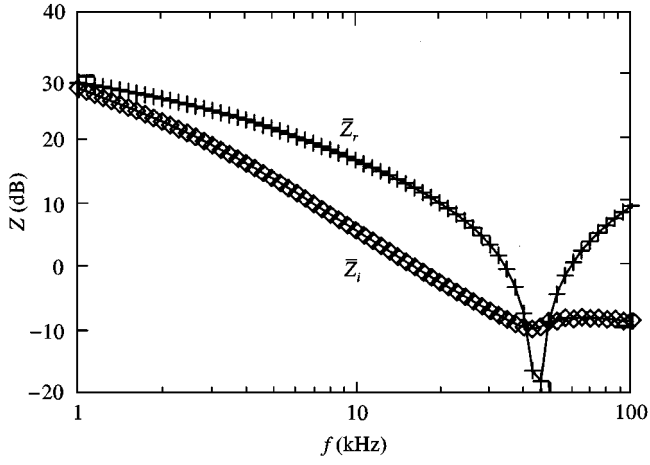

Figure 7. Impedance for full model (◇, +) and low reduced frequency model (—).

It is evident from Figure 7 that both models give the same results for the impedance of the membrane. The other quantities, like velocity and pressure, are also nearly identical. The pressure, for example, does not vary much across the layer thickness: the maximum deviation in the profile is less than 0·1% for frequencies up to 100 kHz. The assumption of constant pressure is reasonable. This is not too surprising when analysing the values of the dimensionless parameters. The conditions $k \ll 1$ and $k/s \ll 1$ hold for the entire frequency range up to 100 kHz: $k < 10^{-1}$ and $k/s < 10^{-2}$. This indicates that the low reduced frequency model will give reliable results, even in the high-frequency range.

In fact, to the author's knowledge, all problems concerning miniaturized transducers that have been presented in the literature could have been solved with the simple low reduced frequency model. None of these cases required the use of the full model. For gases under atmospheric conditions the low reduced frequency model is sufficient and clearly the most efficient.

5. SQUEEZE FILM DAMPING BETWEEN PLATES

As a fourth application, a squeeze film damping problem is analyzed. Consider a flexible plate, located parallel to a fixed surface (see Figure 8). A thin layer of air is trapped between the vibrating plate and the rigid surface. This problem was solved by Trochidis using a simplified Navier–Stokes model. An uncoupled approach was used: the vibrational behaviour of the plate was imposed as a boundary condition for the fluid. The results of this model will now be compared with the results from a low reduced frequency model.

The plate properties are: thickness t_p, density ρ_p and Young's modulus E_p. The problem to be considered is two dimensional: there is no variation in the y-direction. The deflection of the plate is imposed as a boundary condition for the fluid. The velocity, imposed by Trochidis, can be written as

$$\bar{v}_p = c_0 v_p \cos(k_p x) e^{i\omega t}, \tag{44}$$

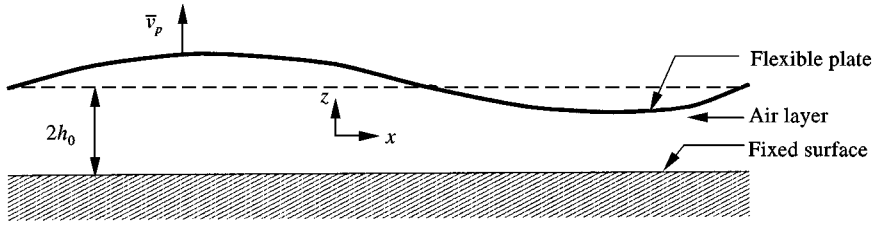

Figure 8. Squeeze film damping problem.

where v_p is the dimensionless amplitude of the velocity (a constant) and k_p is the wave number. According to Trochidis, the wave number is

$$k_p = \frac{c_0}{\omega}\left[\frac{\omega^2 \rho_p t_p}{D_p}\right]^{1/4}\left[1 + \left[\frac{\rho_0}{\rho_p t_p}\right]^{1/4}\right]^{1/5}, \qquad D_p = \frac{E_p t_p^3}{12}. \tag{45}$$

The second term in the expression for k_p accounts for the fact that the free wave number of the plate is affected by the gas or fluid loading on the upper side of the plate. This term can be significant when the plate is loaded with a heavy fluid. For gases, the term can usually be neglected. For the present case the correction is wave number is only 0·1%. Therefore, the wave number is simplified to

$$k_p = \frac{c_0}{\omega}\left[\frac{\omega^2 \rho_p t_p}{D_p}\right]^{1/4}. \tag{46}$$

5.1. SIMPLIFIED NAVIER–STOKES SOLUTION

5.1.1. *Basic equations*

The equations for incompressible behaviour are

$$\Delta p = 0, \qquad [\Delta - \mathrm{i}s^2]\mathbf{v} = \frac{s^2}{k\gamma}\nabla p. \tag{47}$$

5.1.2. *Solution of the equations*

Using separation of variables, one obtains

$$\begin{aligned} p &= [C_1 \mathrm{e}^{-k_{p1}z} + C_2 \mathrm{e}^{k_{p1}z}]\cos(k_p x), \\ \mathbf{v} &= -\frac{s^2}{\gamma}\frac{k_p}{k_{p1}^2 - k_{p2}^2}[C_1 \mathrm{e}^{-k_{p1}z} + C_2 \mathrm{e}^{k_{p1}z}]\sin(k_p x)\mathbf{e}_x \\ &\quad + [C_3 \mathrm{e}^{-k_{p2}z} + C_4 \mathrm{e}^{k_{p2}z}]\sin(k_p x)\mathbf{e}_x \\ &\quad + \frac{s^2}{\gamma}\frac{k_p}{k_{p1}^2 - k_{p2}^2}[C_1 \mathrm{e}^{k_{p1}z} + C_2 \mathrm{e}^{k_{p1}z}]\cos(k_p x)\mathbf{e}_z \\ &\quad + \frac{k_{p1}}{k_{p2}}[C_3 \mathrm{e}^{-k_{p2}z} + C_4 \mathrm{e}^{k_{p2}z}]\cos(k_p x)\mathbf{e}_z, \end{aligned} \tag{48}$$

where the wave numbers k_{p1} and k_{p2} are given by†

$$k_{p1} = kk_p, \qquad k_{p2} = \sqrt{\mathrm{i}s^2 + k^2 k_p^2}. \tag{49}$$

The four constants C_1, C_2, C_3, C_4 are determined from the following boundary conditions: $\mathbf{v}\cdot\mathbf{e}_x = 0$ for $z = \pm 1$; $\mathbf{v}\cdot\mathbf{e}_z = 0$ for $z = -1$; $\mathbf{v}\cdot\mathbf{e}_z = v_p \cos(k_p x)$ for $z = 1$.

5.2. LOW REDUCED FREQUENCY SOLUTION

The equation to be solved is

$$k^2 \frac{\partial^2 p}{\partial x^2} - k^2 \Gamma^2 p = -\mathrm{i}kn(s\sigma)\Gamma^2 \tfrac{1}{2} v_p \cos(k_p x). \tag{50}$$

The solution for an infinite plate is simply

$$p = \frac{\mathrm{i}n(s\sigma)\Gamma^2}{2k[k_p^2 + \Gamma^2]}\, v_p \cos(k_p x). \tag{51}$$

Note that the compressibility effects are accounted for in this expression.

5.3. EXAMPLE: LOSS FACTOR

Trochidis used the loss factor of the system to compare analytical and experimental results. In order to calculate the loss factor, the different forms of energy in the system have to be identified. In the case of compressible behaviour three terms are of interest: the dissipated energy per cycle, $\bar{E}_{diss}$, the maximum elastic energy stored in the plate, $\bar{E}_p$, and the potential energy stored in the air layer, $\bar{E}_{lay}$. For this problem these quantities can be written as

$$\bar{E}_{diss} = -\frac{\pi p_0 c_0}{\omega} \int_A \mathrm{Re}(p v_p^*)\, \mathrm{d}A, \qquad \bar{E}_p = \frac{1}{2} D_p c_0^2 \int_A \left[\frac{\partial^2 v_p}{\partial \bar{x}^2}\right]^2 \mathrm{d}A,$$

$$\bar{E}_{lay} = \frac{1}{2} \frac{p_0^2}{\rho_0 c_0^2} \int_A \int_{\bar{z}=-h_0}^{h_0} [\mathrm{Re}(p)]^2\, \mathrm{d}\bar{z}\, \mathrm{d}A, \tag{52}$$

where A denotes the surface area of the plate and $*$ denotes a complex conjugate. The loss factor is then obtained from

$$\zeta = \bar{E}_{diss}/2\pi[\bar{E}_p + \bar{E}_{lay}]. \tag{53}$$

The following values were used for the present test case:

$$E_p = 70 \times 10^9\ \mathrm{N/m^2}, \qquad t_p = 1 \times 10^{-3}\ \mathrm{m}, \qquad \rho_p = 2710\ \mathrm{kg/m^3},$$
$$\lambda = 25{\cdot}6 \times 10^{-3}\ \mathrm{W/mK}, \qquad \rho_0 = 1{\cdot}2\ \mathrm{kg/m^3}, \qquad C_v = 716\ \mathrm{J/kgK},$$
$$\mu = 18{\cdot}2 \times 10^{-6}\ \mathrm{Ns/m^2}, \qquad C_p = 1004\ \mathrm{J/kgK}, \qquad c_0 = 340\ \mathrm{m/s},$$
$$2h_0 = 1{\cdot}5 \times 10^{-3}\ \mathrm{m}. \tag{54}$$

†Trochidis approximated the wave number k_{p2} by $s\sqrt{\mathrm{i}}$.

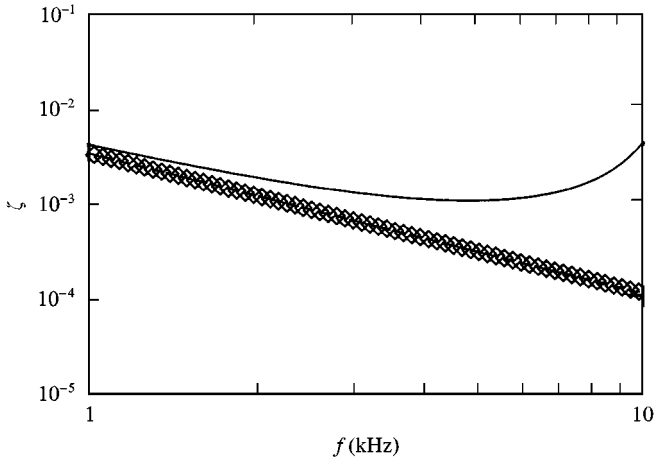

Figure 9. Loss factor versus frequency: Trochidis model (◇), low reduced frequency model (—), incompressible low reduced frequency model (– –).

The loss factor as a function of frequency is given in Figure 9. Results are plotted for the Trochidis model, the low reduced frequency model and the low reduced frequency model for incompressible behaviour.

The figure clearly shows that the Trochidis model and the low reduced frequency model for incompressible behaviour give the same results. The loss factor shows a decrease with increasing frequency for these incompressible models. The low reduced frequency solution including compressibility effects however shows an increasing loss factor for high frequencies.

The increase can be attributed to a coincidence effect. For the present case the acoustic wavelength and the bending wavelength are equal for a frequency just above 10 kHz. For this frequency, energy is radiated efficiently into the layer. Both $\bar{E}_{diss}$ and $\bar{E}_{lay}$ exhibit a peak at this frequency. The final result is a peak in the loss factor. Note that incompressible models are not able to describe the coincidence phenomenon.

The two incompressible models give the same result for the loss factor. For the entire frequency range, the conditions $k \ll 1$ and $k/s \ll 1$ hold: $k < 1$ and $k/s < 10^{-2}$. Therefore, the low reduced frequency assumptions are valid. Again, there is no need to use a more complicated model.

6. NUMERICAL TECHNIQUES

In the previous sections an overview was presented of analytical solutions for viscothermal wave propagation, including acousto-elastic interaction. In general, analytical solutions can be found only for simple geometries and boundary conditions. For more complex situations numerical solution procedures are necessary.

Recently, a boundary element formulation for viscothermal wave propagation in thin layers was presented by Karra *et al.* [17] and Karra and Ben Tahar [18]. This

model is based on the full linearized Navier–Stokes model. The boundary element model is able to deal with coupled calculations for rotatory symmetric problems. In part I of the present paper however it was demonstrated that the full linearized Navier–Stokes model has to be used only under extreme conditions. In most cases, the simple low reduced frequency model is sufficient to describe viscothermal wave propagation.

A low reduced frequency approach was described for instance by Fox and Whitton [19], Önsay [20, 21] and Beltman *et al.* [22, 23]. Fox and Whitton adopted an analytical approach, while Önsay developed a transfer matrix approach. These techniques are only suited for simple geometries. The paper by Beltman *et al.* describes a finite element approach. As a first step, the low reduced frequency model was validated by means of special experiments with an oscillating solar panel [22]. A viscothermal acoustic finite element was developed to describe the pressure distribution in thin layers or narrow tubes. The new viscothermal acoustic finite element can be coupled to a structural finite element, enabling fully coupled acousto-elastic calculations for complex geometries. The model was experimentally validated by means of experiments on an airtight box with a flexible coverplate [23]. The new elements were successfully used to analyze the dynamical behaviour of solar panels during launch, to predict the damping capabilities of the double-wall panels and to predict the dynamical behaviour of an inkjet printhead [24].

7. CONCLUSIONS

The conclusions to be drawn from the present investigations are as follows,

Analytical solutions of the full linearized Navier–Stokes model and the low reduced frequency model were presented for various geometries. Because all the solutions are written in terms of dimensionless parameters, the ranges of validity can be indicated.

The low reduced frequency model is sufficient and the most efficient to describe viscothermal wave propagation for the majority of problems.

Efficient finite element models, based on the low reduced frequency model, are available to deal with fully coupled acousto-elastic calculations involving viscothermal wave propagation, complex geometries and complex boundary conditions.

ACKNOWLEDGMENTS

The author would like to thank Henk Tijdeman, Ruud Spiering, Peter van der Hoogt, Bert Wolbert, Tom Basten, Frits van der Eerden, Diemer de Vries, Leen van Wijngaarden, Jan Verheij, Piet Zandbergen, Jean Pierre Coyette and Bart Paarhuis for their valuable suggestions and comments.

REFERENCES

1. M. Moldover, J. Mehl and M. Greenspan 1986 *Journal of the Acoustical Society of America* **79**, 253–270. Gas-filled spherical resonators: theory and experiment.

2. M. Bruneau, J. D. Polack, Ph. Herzog and J. Kergomard 1990 *Colloque de Physique* **51**, C2-17–C2-20. Formulation générale des équations de propagation et de dispersion des ondes sonores dans les fluides viscothermiques [in French].
3. M. Bruneau, Ph. Herzog, J. Kergomard and J. D. Polack 1989 *Wave Motion* **11**, 441–451. General formulation of the dispersion equation in bounded visco-thermal fluid.
4. J. B. Mehl 1985 *Journal of the Acoustical Society of America* **78**, 782–788. Spherical acoustic resonator: effects of shell motion.
5. J. B. Mehl 1982 *Journal of the Acoustical Society of America* **71**, 1109–1113. Acoustic resonance frequencies of deformed spherical resonators.
6. J. B. Mehl 1986 *Journal of the Acoustical Society of America* **79**, 278–285. Acoustic resonance frequencies of deformed spherical resonators, II.
7. M. Abramowitz and I. A. Stengun *Handbook of Mathematical Functions*. New York: Dover publications, seventh edition.
8. P. M. Morse and H. Feshbach 1953 *Methods of Theoretical Physics*. New York: McGraw-Hill.
9. J. W. S. Rayleigh 1945 *The Theory of Sound*, Vol. New York: Dover publications second, revised edition.
10. H. Tijdeman 1975 *Journal of Sound and Vibration* **39**, 1–33. On the propagation of sound waves in cylindrical tubes.
11. P. N. Liang and H. A. Scarton 1996 *Journal of Sound and Vibration* **193**, 1099–1113. Attenuation of higher order circumferential thermoacoustic waves in viscous fluid lines.
12. P. N. Liang and H. A. Scarton 1994 *Journal of Sound and Vibration* **177**, 121–135. Three-dimensional mode shapes for higher order circumferential thermoelastic waves in an annular elastic cylinder.
13. H. Hudde 1988 *Journal of the Acoustical Society of America* **83**, 1311–1318. The propagation constant in lossy circular tubes near the cutoff frequencies of higher order modes.
14. A. M. Bruneau, M. Bruneau, Ph. Herzog and J. Kergomard 1987 *Journal of Sound and Vibration* **119**, 15–27. Boundary layer attenuation of higher order modes in waveguides.
15. J. Kergomard, M. Bruneau, A. M. Bruneau and Ph. Herzog 1988 *Journal of Sound and Vibration* **126**, 178–181. On the propagation constant of higher order modes in a cylindrical waveguide.
16. G. Plantier and M. Bruneau 1990 *Journal Acoustique* **3**, 243–250. Heat conduction effects on the acoustic response of a membrane separated by a very thin air film from a backing electrode.
17. C. Karra, M. B. Tahar, G. Marquette and M. T. Chau *InterNoise* **96**, 3003–3006 Liverpool, United Kingdom 1996. (F. Allison Hill and R. Lawrence editors). Boundary element analysis of problems of acoustic propagation in viscothermal fluid.
18. C. Karra and M. Ben Tahar 1997 *Journal of the Acoustical Society of America* **102**, 1311–1318. An integral equation formulation for boundary element analysis of propagation in viscothermal fluids.
19. M. J. H. Fox and P. N. Whitton 1980 *Journal of Sound and Vibration* **73**, 279–295. The damping of structural vibrations by thin gas films.
20. T. Önsay 1993 *Journal of Sound and Vibration* **163**, 231–259. Effects of layer thickness on the vibration response of a plate-fluid layer system.
21. T. Önsay 1994 *Journal of Sound and Vibration* **178**, 289–313. Dynamic interaction between the bending vibrations of a plate and a fluid layer attenuator.
22. W. M. Beltman, P. J. M. van der hoogt, R. M. E. J. Spiering and H. Tijdeman 1997. *Journal of Sound and Vibration* **206**, 217–241. Air loads on a rigid plate oscillating normal to a fixed surface.

23. W. M. Beltman, P. J. M. van der hoogt, R. M. E. J. Spiering and H. Tijdeman 1998. *Journal of Sound and Vibration* **216**, 159–185. Implementation and experimental validation of a new viscothermal acoustic finite element for acousto-elastic problems.
24. W. M. Beltman 1998 *Ph.D. thesis University of Twente, Department of Mechanical Engineering, The Netherlands.* Viscothermal wave propagation including acousto-elastic interaction. ISBN 90-3651217-4.

APPENDIX: NOMENCLATURE

A_q, B_q	participation factors
$A_{aq}, B_{aq}, A_{hq}, B_{hq}$	constants
$B(s)$	function accounting for viscous or thermal effects
$a = l_y/l_x$	aspect ratio
C_1, C_2, C_3, C_4	constants
C_p	specific heat at constant pressure
C_v	specific heat at constant volume
c_0	undisturbed speed of sound
$D_p = E_p t_p^3/12$	bending stiffness
E_p	Young's modulus of plate material
$\bar{E}_{diss}$	dissipated energy per cycle
$\bar{E}_{in}$	incident energy per cycle
$\bar{E}_{lay}$	energy stored in the air layer
$\mathbf{e}_n$	unit normal vector
$\mathbf{e}_r$	unit vector in the r-direction
$\mathbf{e}_x$	unit vector in the x-direction
$\mathbf{e}_y$	unit vector in the y-direction
$\mathbf{e}_z$	unit vector in the z-direction
$\mathbf{e}_\theta$	unit vector in the θ-direction
$\mathbf{e}_\phi$	unit vector in the ϕ-direction
f_m	function describing wave propagation in tubes
h_0	half-layer thickness
$\mathrm{i} = \sqrt{-1}$	imaginary unit
j_n	spherical Bessel function of order n
J_m	Bessel function of the first kind, order m
$k = \omega l/c_0$	reduced frequency
k_a	acoustic wave number
$k_{aq} = k_a^2 - k_q^2$	wave number
$k_{ar} = \sqrt{k_a^2 + k^2\Gamma^2}$	wave number
k_h	entropic wave number
$k_{hq} = k_h^2 - k_q^2$	wave number
$k_{hr} = \sqrt{k_h^2 + k^2\Gamma^2}$	wave number
k_p	plate elastic wave number
$k_{p1} = kk_p$	wave number
$k_{p2} = \sqrt{\mathrm{i}s^2 + k^2k_p^2}$	wave number
k_q	wave number
$k_r = \omega R/c_0$	wave number in the r-direction
$k_x = \omega l_x/c_0$	wave number in the x-direction
k_v	rotational wave number
$k_{vq} = k_v^2 - k_q^2$	wave number
l	characteristic length scale
l_x	half-length in the x-direction
l_y	half-length in the y-direction

l_z	half-length in the z-direction
m	order of circumferential harmonic waves
$n(s\sigma)$	polytropic constant
$\bar{p} = p_0[1 + p\mathrm{e}^{\mathrm{i}\omega t}]$	pressure
p_0	mean pressure
p	dimensionless pressure amplitude
$\bar{p}_i = p_0[1 + p_i\mathrm{e}^{\mathrm{i}\omega t}]$	incident pressure on membrane
p_i	dimensionless incident pressure amplitude
R	radius
R_0	gas constant
$\bar{r}$	radial co-ordinate
r	dimensionless radial co-ordinate
$s = l\sqrt{\rho_0\omega/\mu}$	shear wave number
$\bar{T} = T_0[1 + T\mathrm{e}^{\mathrm{i}\omega t}]$	temperature
T_0	mean temperature
T	dimensionless temperature amplitude
T_a	acoustic temperature
T_h	entropic temperature
T_m	membrane tension
t	time
t_m	membrane thickness
t_p	plate thickness
$\bar{\mathbf{v}} = c_0\mathbf{v}\mathrm{e}^{\mathrm{i}\omega t}$	velocity vector
$\mathbf{v}$	dimensionless amplitude of the velocity vector
v	dimensionless amplitude of the velocity
$\mathbf{v}_l$	solenoidal velocity vector
$\mathbf{v}_{la}$	acoustic part of solenoidal velocity vector
$\mathbf{v}_{lh}$	entropic part of solenoidal velocity vector
$\mathbf{v}_v$	rotational velocity vector
$\bar{v}_m = c_0 v_m \mathrm{e}^{\mathrm{i}\omega t}$	membrane velocity
$\langle \bar{v}_m \rangle$	average membrane velocity
v_m	dimensionless membrane velocity
$\bar{v}_p$	plate velocity
v_p	dimensionless plate velocity
v_r	dimensionless velocity component in the r-direction
$\bar{v}_{ref}$	reference velocity
v_x	dimensionless velocity component in the x-direction
$\bar{v}_{xn}$	nozzle velocity in the x-direction
v_{xn}	dimensionless nozzle velocity in the x-direction
v_y	dimensionless velocity component in the y-direction
v_z	dimensionless velocity component in the z-direction
v_θ	dimensionless velocity component in the θ-direction
v_ϕ	dimensionless velocity component in the ϕ-direction
W_1, W_2	constants
$\bar{x} = l_x x$	x-co-ordinate
x	dimensionless x-co-ordinate
$\mathbf{x}$	spatial co-ordinates
$\bar{y} = l_y y$	y-co-ordinate
Y_{mn}	spherical harmonic function
y	dimensionless y-co-ordinate
$\bar{z} = h_0 z$	z-co-ordinate
$\bar{Z}$	membrane impedance
$\bar{Z}_0$	reference level for the impedance
$\bar{Z}_i$	imaginary part of membrane impedance

Z_n	specific normal acoustic impedance
$\bar{Z}_r$	real part of membrane impedance
z	dimensionless z-co-ordinate
Γ	propagation constant
$\gamma = C_p/C_v$	ratio of specific heats
$\varepsilon = \rho_0 h_0/\rho_p t_p$	ratio of mass per unit area
η	bulk viscosity
$\bar{\theta}$	co-ordinate in the θ-direction
θ	dimensionless co-ordinate in the θ-direction
Λ_a	constant
Λ_h	constant
λ	thermal conductivity
μ	dynamic viscosity
ξ	viscosity ratio
ν_p	Poisson's ratio of plate material
$\bar{\rho} = \rho_0[1 + \rho e^{i\omega t}]$	density
ρ_0	mean density of air
ρ	dimensionless density amplitude
ρ_m	density of membrane material
ρ_p	density of plate material
$\sigma = \sqrt{\mu C_p/\lambda}$	square root of the Prandtl number
$\bar{\phi}$	co-ordinate in the ϕ-direction
ϕ	dimensionless co-ordinate in the ϕ-direction
Ω	dimensionless frequency
ω	angular frequency
$\bar{\mathbf{V}}$	gradient operator
$\mathbf{V}$	dimensionless gradient operator
$\bar{\Delta}$	Laplace operator
Δ	dimensionless Laplace operator
Δ^{cd}	dimensionless Laplace operator in the cd-directions
Δ^r	dimensionless Laplace operator in the r-direction
ζ	loss factor
*	complex conjugate